

Clinical Evaluation of Fast T2-Corrected MR Spectroscopy Compared to Multi-Point 3D Dixon for Hepatic Lipid and Iron Quantification

Puneet Sharma¹, Xiaodong Zhong², Jean-Philippe Galons³, Bobby Kalb³, Maria Altbach³, and Diego R Martin³

¹Medical Imaging, University of Arizona, Tucson, Arizona, United States, ²MR R&D Collaborations, Siemens Healthcare, Atlanta, GA, United States, ³Medical Imaging, University of Arizona, Tucson, AZ, United States

Target Audience: Translational Scientists, Body Radiologists, Sequence Developers

Background: Advanced MR imaging, using multi-point Dixon reconstruction, allows 3-dimensional assessment of hepatic fat fraction (FF) and local R2*, which is a surrogate for iron concentration (1-5). In addition, a high-speed, T2-corrected single-voxel spectroscopy (HISTO-MRS) approach has been developed to interrogate hepatic water and lipid compartments, and to elucidate FF and R2 values of these components in a single breath hold (6). Thus far, this fast single breath-hold HISTO-MRS has not been formally evaluated in the clinical environment, nor compared to current 3D multi-point Dixon imaging in terms of lipid and iron estimation.

Purpose: 1) To evaluate breath hold HISTO-MRS in a routine clinical environment, in consecutive patients; 2) To correlate hepatic FF from HISTO-MRS and 3D multi-point Dixon at 1.5T; and 3) to compare HISTO-R2 measures with R2* for sensitivity to iron content.

Methods: This investigation was approved by the IRB, was HIPPA-compliant, and all participants signed informed consent prior to imaging. All imaging was performed on a Siemens 1.5T Aera system using an 18-channel phased-array body coil. Thirty-nine consecutive patients arriving for routine abdominal MRI over a two week period were recruited for this study. The exclusion criteria consisted of standard MR contraindications. Each patient received two additional breath hold acquisitions: 1) single-voxel HISTO-MRS; and 2) 6-point 3D GRE (3D Dixon FQ). The HISTO-MRS voxel was prescribed using available T2-weighted single-shot localizer acquisitions. The voxel was placed in a region free of major hepatic vessels, usually in the right lobe. The MRS parameters were: STEAM sequence; TR/TM = 3000ms/10ms; 5 TEs = {12, 24, 36, 48, 72}ms; voxel = 20-30mm³; 1 signal average; time = 15sec. The 3D Dixon FQ sequence consisted of 80 slices prescribed to cover the full liver volume. Other parameters included: TR = 9.1ms; 6 TEs = 1.2/2.5/3.7/5.0/6.3/7.6ms; matrix = 256 x 154; FOV = 400-420mm; phase FOV = 75%; slice thickness = 3mm; BW = 1085Hz/px; time = 18sec. Post-processing for both techniques were performed automatically at the scanner console with inline reconstruction. For HISTO-MRS, the integral signal area of both water and total lipid (-1.3 ± 0.8 ppm) spectra were automatically tabulated at each TE, whereby T2 of both components ($R2_{water}$ and $R2_{lipid}$) were quantified using a non-linear least squares algorithm, and a goodness-of-fit measure (r^2). The fat fraction (FF_{HISTO}) was calculated from the ratio of T2-corrected lipid integral to T2-corrected lipid + water integral (1). Using a multi-step fitting approach, the 3D Dixon FQ data was processed automatically by fitting the multi-echo data to the magnitude of the complex signal model that included the coefficients and frequency components for a seven-peak fat model (5). Volumetric T2*-corrected fat fraction (FF_{DIXON}) maps were calculated from the fitting, along with R2* maps. **Analysis:** Mean and standard deviation measurements of FF_{DIXON} and R2* were performed in Clear Canvas Workstation 2.0 (Toronto, CA) from region-of-interests (ROIs) in approximate region of the HISTO-MRS voxel. Agreement of FF_{HISTO} and FF_{DIXON} was performed with Bland-Altman analysis, with measures of bias and 95% confidence limits. Since R2* has been shown to correlate with hepatic iron content (7), Pearson correlation was performed against both $R2_{water}$ and $R2_{lipid}$. Significance was set to $p < 0.05$.

Results: All patients tolerated the additional MR acquisitions. 1/39 patients were excluded due to large metal artifact, 3/39 3D Dixon FQ cases experienced fat-water “swap”, leading to uncalculated R2* maps, while 1/39 HISTO-MRS case suffered from poor T2 fit ($r^2 < 0.6$) due to severe iron deposition. Therefore, 34 patients were included in the analysis. For low FF_{HISTO} ($< 6.0\%$, $n=22$), $R2_{lipid}$ could not be reliably calculated due to poor lipid SNR. Figure 1 shows representative HISTO-MRS spectra and corresponding FF_{DIXON} and R2* maps in one patient. Figure 2 shows the Bland-Altman plot comparing FF_{HISTO} and FF_{DIXON} . The bias was -0.5% , and 95% confidence was $\pm 4.8\%$, which represents a significant correlation ($r=0.99$, $p < 0.01$), despite 1 outlier at high FF (red circle in Fig. 2). $R2_{water}$ measurement from HISTO-MRS correlated significantly with R2* ($r=0.87$, $p < 0.01$), while $R2_{lipid}$ did not correlate ($r=0.12$, $p=0.5$), and remained relatively constant in patients with elevated FF ($R2_{lipid} = 20.5 \pm 4.1\%$, $FF > 8.0\%$, $n=7$).

Discussion: With automatic post-processing, HISTO-MRS was efficiently performed in a routine clinical setting. Significant agreement in FF was found between HISTO-MRS and 3D Dixon FQ. From the behavior of $R2_{water}$ and $R2_{lipid}$, the results also confirm that hepatic iron content affects $R2_{water}$ compartment more significantly than $R2_{lipid}$. Limitations of the current HISTO-MRS include poor estimation of severe iron deposition (due to long initial TE) and unreliable $R2_{lipid}$ for low FF_{HISTO} .

Conclusions: Both HISTO-MRS and 3D Dixon FQ are viable clinical methods for the estimation of hepatic fat fraction (FF) and iron content (R2* and $R2_{water}$).

References: 1. Chebrulov et al. Magn Reson Med 2010;63:849-857; 2. Hernando et al. Magn Reson Med 2010;63:79-90; 3. Bydder et al. Magn Reson Imaging 2008;26:347-359; 4. Yu et al. Magn Reson Med 2011;66:199-206; 5. Zhong et al. Magn Reson Med; in press; 6. Pineda et al. Radiology 2009;252:568-576; 7. Wood et al. Blood 2005;106:1460-1465.

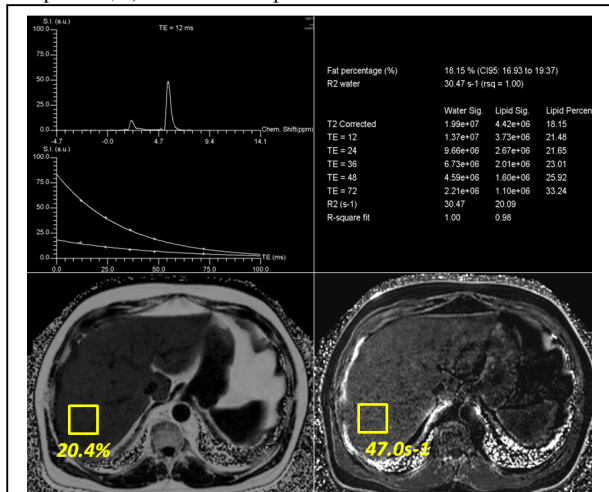


Figure 1. HISTO report (top) and Dixon FQ maps (bottom)

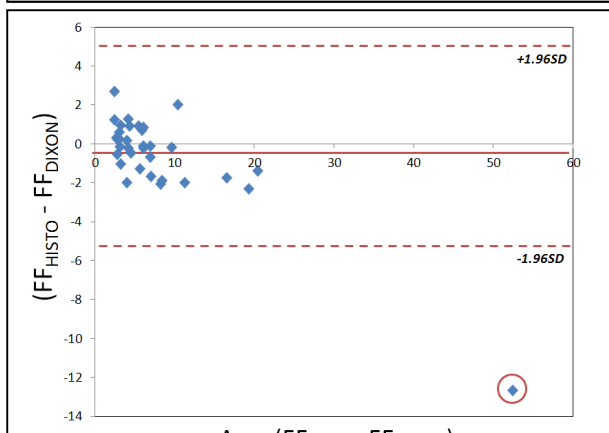


Figure 2. Bland-Altman analysis of FF.